

# Dual-frequency radar ratio of nonspherical atmospheric hydrometeors

S. Y. Matrosov,<sup>1</sup> A. J. Heymsfield,<sup>2</sup> and Z. Wang<sup>3</sup>

Received 12 April 2005; revised 23 May 2005; accepted 8 June 2005; published 9 July 2005.

[1] Dual-frequency cloud and precipitation radar systems are being actively developed and installed on different platforms. The use of two radar frequencies (with at least one frequency outside the Rayleigh type of scattering for hydrometeors of interest) allows independent estimates of hydrometeor effective size. With these estimates, radar-based retrievals of such important parameters as cloud mass content or precipitation rate can be potentially performed with better accuracy compared to single-frequency radar measurements. This study presents quantitative assessments of the effects of nonsphericity of ice cloud particles which influence the dual-frequency ratio used for characteristic size estimates. **Citation:** Matrosov, S. Y., A. J. Heymsfield, and Z. Wang (2005), Dual-frequency radar ratio of nonspherical atmospheric hydrometeors, *Geophys. Res. Lett.*, **32**, L13816, doi:10.1029/2005GL023210.

## 1. Introduction

[2] Dual- (and multi-) frequency radar measurements are increasingly used for remote sensing of ice hydrometeors from the ground [e.g., Matrosov, 1992, 1998; Sekelsky *et al.*, 1999; Hogan *et al.*, 2000] and, more recently, from the airborne platforms [e.g., Heymsfield *et al.*, 2005; L. Liao *et al.*, Validation of snow parameters as derived from dual-wavelength airborne radar, preprints from 31st Conference on Radar Meteorology, American Meteorological Society, Seattle, Washington, 2003, hereinafter referred to as Liao *et al.*, unpublished manuscript, 2003]. Meteorological radars typically operate at S, C, X, Ku, Ka and W bands which correspond to frequencies at around 3, 5, 10, 17, 35 and 94 GHz, respectively. Under the Rayleigh conditions, when scattering particles are much smaller than radar wavelengths  $\lambda$ , backscatter coefficients,  $\eta$ , at different frequencies are scaled as the fourth power of wavelength  $\lambda^4$ , and the corresponding equivalent radar reflectivity factors,  $Z_e$  defined as:

$$Z_e = \lambda^4 \pi^{-5} |(m^2 + 2)/(m^2 - 1)|^2 \eta \quad (1)$$

vary little with wavelength ( $m$  is the complex refractive index of water at a given frequency).

[3] When the Rayleigh conditions are not satisfied at least at one frequency,  $v_2 (v_2 > v_1)$ , reflectivity factors differ,

and their logarithmic difference, defined as the dual frequency ratio (DFR)

$$\text{DFR} = 10 \cdot \log_{10}[Z_e(v_1)] - 10 \cdot \log_{10}[Z_e(v_2)] \quad (2)$$

can be used for inferring a characteristic particle size. For populations of particles, DFR usually increases as particles grow larger.

[4] In most recent studies, DFR values were modeled using a spherical particle assumption, though some theoretical studies [e.g., Matrosov, 1993] point to the dependence of DFR on particle shapes. The use of spherical shape is usually justified by the relative simplicity of calculations and the lack of information on the exact shape of the particles. Besides, under the Rayleigh conditions, the difference between backscatter of spherical and equal-volume nonspherical particles is generally within 1–1.5 dB or so [Atlas *et al.*, 1953] which is close to the uncertainty of reflectivity measurements.

[5] For dual-frequency measurements, however, scatterer nonsphericity could be more important to account for compared to single reflectivity data. In part, this is because DFR varies in a relatively narrow range, so even small uncertainties in DFR can be important. This study presents theoretical estimates of DFR for experimental ice particle distributions depending on particle nonsphericity. The model results are then compared to coincident airborne radar measurements at frequencies of 9.6 and 94 GHz. These comparisons indicate the importance for accounting of particle nonsphericity when inferring a characteristic particle size from nadir-viewing dual-frequency radar data.

## 2. Computational Model

[6] A number of different methods has been suggested for calculating scattering properties (such as  $\eta$ ) of nonspherical particles [Mishchenko *et al.*, 2000]. One of those methods, namely the T-matrix method [Barber and Yeh, 1975] as applied to spheroidal shapes, proved to be particularly useful for modeling nonspherical hydrometeors at radar frequencies. At these frequencies, the sizes of most atmospheric hydrometeors (expressed by their major dimensions,  $D$ ) are either much smaller than radar wavelengths (i.e., the Rayleigh scattering regime) or these sizes are approaching the radar wavelengths, however, usually still remaining smaller than  $\lambda$  (e.g., larger ice cloud particles, snowflakes, and raindrops at W and, to a certain extent, Ka-band frequencies). At such size-wavelength correspondences, the subtle differences in particle shapes are relatively unimportant, and scattering properties depend mostly on the overall shape [Dungey and Bohren, 1993] as determined by the particle aspect ratio,  $r$ , (i.e., minor-to-major dimension ratio).

[7] The spheroidal model was shown to adequately describe radar polarization backscatter properties of most

<sup>1</sup>Cooperative Institute for Research in Environmental Sciences, University of Colorado and NOAA ETL, Boulder, Colorado, USA.

<sup>2</sup>National Center for Atmospheric Research, Boulder, Colorado, USA.

<sup>3</sup>Department of Atmospheric Sciences, University of Wyoming, Laramie, Wyoming, USA.

atmospheric hydrometeors including ice cloud particles, pristine snowflakes, and raindrops [e.g., *Bringi and Chandrasekar*, 2001; *Matrosov et al.*, 2001]. It is expected to be appropriate for modeling DFR properties. Another convenience of the spheroidal model and the T-matrix computational method for studies performed here is that for the spherical shape ( $r = 1$ ), the T-matrix solution reduces to the well-known Mie solution for spheres.

[8] The smallest ice cloud particles with sizes less than about 50  $\mu\text{m}$  are usually quasi-spherical. Contributions of such particles to the reflectivity are usually negligible for particle populations with characteristic sizes greater than about 100  $\mu\text{m}$ . *Korolev and Isaac* [2003] presented the analysis of shapes for ice cloud particles with  $D > 60 \mu\text{m}$ . They found that the ratio  $D_w/D$  ( $D_w$  is the particle dimension in the direction perpendicular to its maximum dimension) does not significantly depend on  $D$  and is about 0.6–0.8. At the same time, the ratio of the particle cross-sectional area to that of a spherical particle with diameter  $D$  shows some decreasing trend with increasing  $D$ . To simplify DFR modeling, it was assumed here that for the chosen spheroidal model, the aspect ratio does not change with particle size  $D$ . At this stage such an assumption is, probably, justified for the spheroidal model adopted here.

### 3. Ice Cloud Experimental Data

[9] Coincident airborne radar and in situ cloud microphysical data were collected during the Cirrus Regional Study of Tropical Anvils and Cirrus Layers (CRYSTAL) Florida Area Cirrus Experiment (FACE) in southern Florida in July 2002. The dual-frequency radar ( $\nu_1 = 9.6 \text{ GHz}$ ,  $\nu_2 = 94 \text{ GHz}$ ) was deployed onboard a NASA ER-2 aircraft flying at 20 km altitude. Simultaneously, the University of North Dakota Citation aircraft flew directly underneath the ER-2. Two-dimensional ice cloud particle size distributions (PSDs) in 33 size bins covering a range from 30  $\mu\text{m}$  to 2.5 mm were collected by the Citation aircraft [*Heymsfield et al.*, 2005].

[10] The in situ microphysical data were practically coincident with radar measurements from the ER-2 at the Citation altitude. The mean horizontal spatial distance between the ER-2 and Citation was  $0.69 \pm 1.13 \text{ km}$ , and the mean time difference between the radar and in situ microphysical data was  $33 \pm 52 \text{ sec}$ . To minimize the ER-2 and Citation spatial and temporal sampling differences, reflectivity data were obtained at two points within a few seconds before and two points within a few seconds after what was deemed to be the exact position of the Citation aircraft [*Heymsfield et al.*, 2005]. These four data points were averaged to represent the reflectivity measurement corresponding to any given PSD measurement.

[11] The in situ PSDs from the Citation aircraft were used to calculate values of  $Z_e(9.6 \text{ GHz})$  and  $Z_e(94 \text{ GHz})$  using the oblate particle spheroidal model and the T-matrix method as discussed above. These calculations require knowledge of the particle density which is computed using the particle mass. This mass,  $m$ , is typically given in terms of a power-law with respect to the particle major dimension,  $D$ :

$$m(g) = a D^b(\mu\text{m}) \quad (3)$$

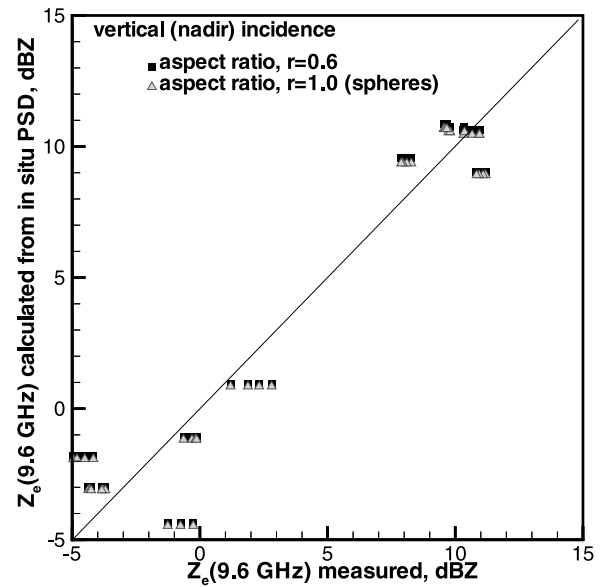


**Figure 1.** Comparisons of measured and calculated values of  $Z_e(9.6 \text{ GHz})$ .

If a value from (3) exceeds the mass of the solid ice particle of a given shape and size, the solid ice mass is used in calculations. *Heymsfield et al.* [2005] investigated the suitability of different mass-size relations for the CRYSTAL-FACE data set and determined that the relation with  $a \approx 1.2 \cdot 10^{-11}$  and  $b \approx 2.1$  suggested by *Mitchell* [1996] provided a good agreement between calculated and measured values of reflectivities at 9.6 GHz (though it was not a case for ice water content calculations).

### 4. Comparisons for Ice Clouds

[12] Figure 1 shows comparisons of reflectivities calculated from PSDs and those measured at the 9.6 GHz frequency. Particles were assumed to be randomly oriented with their major dimensions in the horizontal plane. Such nonspherical particle orientations, explained by the aerodynamic forcing, are often observed with the use of polarimetric measurements [*Matrosov et al.*, 2005]. The mass of individual particles is preserved when switching from the spherical model to the nonspherical one.

[13] Results in Figure 1 show that nonsphericity of particles (aspect ratio  $r = 1$  vs.  $r = 0.6$ ) causes only slight impact on reflectivities at 9.6 GHz (the Rayleigh-type scattering). For a shorter wavelength, where for larger particles scattering deviates from the Rayleigh type, the effects of particle nonsphericity are stronger. This can be seen from Figure 2, where the DFRs computed from in situ data are plotted as a function of the median volume particle size,  $D_o$ , which was also estimated from the in situ PSDs. Note that unlike for absolute values of reflectivities, the DFR-  $D_o$  relation is not very sensitive to the assumption about particle mass-size relation (3) [*Matrosov*, 1998; *Hogan et al.*, 2000; *Liao et al.*, unpublished manuscript, 2003], so there is little compromise about the assumption involving coefficients  $a$  and  $b$  in (3).

[14] As one can see from Figure 2, DFR for nonspherical particles is smaller than that for spheres. For PSDs with

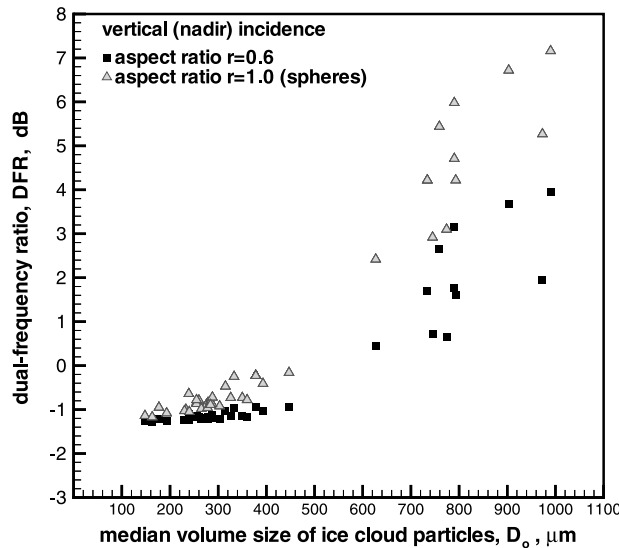


**Figure 2.** DFRs calculated from in situ PSDs as a function of  $D_o$ .

small values of  $D_o$ , where the assumption of the Rayleigh-type scattering is valid for both frequencies, DFR is approaching  $-1.2$  dB (not  $0$  dB) due to differences in the normalizing factor  $|(m^2 + 2)/(m^2 - 1)|^2$  at  $9.6$  and  $94$  GHz. The group of data points with  $D_o < 500$   $\mu\text{m}$  in Figure 2 corresponds to the group of data points with  $Z_e(9.6 \text{ GHz}) < 3$  dBZ. DFR values for these points differ from the limiting value of  $-1.2$  dB insignificantly, and probably cannot be measured accurately enough for sensible estimations of  $D_o$ . PSDs with  $D_o > 600$   $\mu\text{m}$ , corresponding here to  $Z_e(9.6 \text{ GHz}) > 7$  dBZ (see Figure 1), produce sizable DFRs and their characteristic size (i.e.,  $D_o$ ) can be potentially estimated from dual-frequency radar measurements.

[15] DFR data can potentially be more accurate than absolute reflectivity data because DFR measurements can be calibrated in a relative sense. It is known that particle sizes near the upper cloud boundaries are usually small, so one would expect DFRs there to be approaching the theoretical limit which is about  $-1.2$  dB for the given pair of radar frequencies. There are caveats for using DFR data due to differing attenuation rates of radar signals at different frequencies as they propagate through the atmosphere. This differential attenuation effect, however, is expected to be small for airborne measurements above liquid clouds and most of the water vapor. Absorption of radar signals in ice clouds is negligible, though attenuation due to volume scattering needs to be accounted for.

[16] Figure 3 shows the DFR calculations for  $D_o > 600$   $\mu\text{m}$  superimposed by ER-2 DFR measurements for coincident data points. The best linear fits are also plotted for spherical ( $r = 1$ ) and nonspherical ( $r = 0.6$ ) particle models:

$$\text{DFR}(\text{dB}) = -1.0 - 7.1 \cdot 10^{-3} D_o(\mu\text{m}) (r = 0.6) \quad (4)$$

$$\text{DFR}(\text{dB}) = -1.2 - 4.2 \cdot 10^{-3} D_o(\mu\text{m}) (r = 1).$$

For the relatively small dynamic range of  $D_o$  values ( $600 \mu\text{m} < D_o < 1000 \mu\text{m}$ ) and the observed data scatter, simple linear fits are probably appropriate here, and more sophisticated approximation procedures are unnecessary.

[17] The results of nonspherical particle modeling agree better with the ER-2 measurements of DFR in Figure 3. The majority of the experimental DFR points, however, would be better explained by calculations with an aspect ratio of about  $r = 0.7$ ; though, given the relative scarcity of data points and model uncertainties, this result is more qualitative than quantitative. The presented analysis, however, points to the importance of accounting for ice hydrometeor nonsphericity when interpreting DFR measurements in the nadir (or zenith) direction. Using the spherical model for retrieving characteristic particle size from DFR measurements may result in substantial underestimation bias in the results (as much as a factor of 2).

[18] These results also have potential implications for the single-frequency  $94$  GHz spaceborne radar (CloudSat) [Stephens and the CloudSat Science Team, 2002]. It follows from the results presented here that, while particle nonsphericity effects are small for Rayleigh-type scattering, they become increasingly more important as characteristic cloud particle size increases. For  $D_o > 600$   $\mu\text{m}$ , reflectivity of cloud particles with a typical aspect ratio of about  $0.6$  could be several decibels higher than that for equal-volume (mass) spheres. As a result, some biases in the retrieved cloud parameters may be obtained if the retrieval methods have been developed with the use of the spherical particle model.

[19] Modeling was also performed for the horizontal incidence of radar signals assuming the same particle orientation with their major dimension in the horizontal plane. Nonspherical shape effects were significantly more modest for this geometry and the horizontally polarized radar signals than in the case of vertical incidence. This result justifies, in some way, the spherical assumption for low-elevation DFR radar measurements (at least for the frequency pair considered here).

## 5. $K_u$ - $K_a$ -Band Dual-Frequency Ratio for Raindrops

[20]  $K_u$ - $K_a$ -band DFR for raindrops is of particular interest because a spaceborne radar with these frequencies is

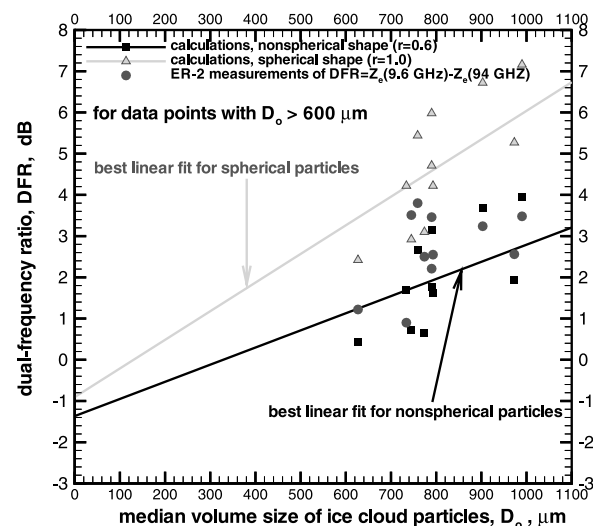


**Figure 3.** DFR as a function of particle median size  $D_o$  as resulting from calculations and measurements.



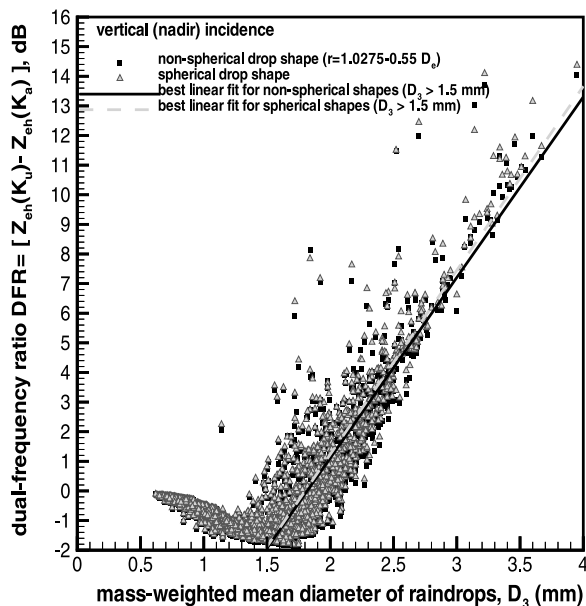


Figure 4.  $K_u$ - $K_a$ -band DFR of rain at vertical incidence.

planned for the Global Precipitation Measurement (GPM) mission [Iguchi *et al.*, 2002]. Figure 4 shows the vertical incidence unattenuated DFR as a function of mass-weighted mean drop diameter,  $D_3$ , calculated for more than 3000 experimental drop size distributions (DSDs) that were obtained in projects described by Matrosov [2005]. These DSDs were collected in a variety of temperature regimes and rain types (e.g., convective vs. stratiform). The nonspherical drop model used here was close to the equilibrium drop model and assumed that drops larger than 500  $\mu\text{m}$  are nonspherical with the aspect ratio linearly depending on the diameter of the equal-volume sphere  $D_e$ .

[21] It can be seen from Figure 4, that raindrop nonsphericity affects DFR at vertical incidence only slightly, and probably can be neglected for most practical cases. There is significant scatter in data points indicating a relatively high uncertainty of using DFR to infer characteristic drop diameter. Significant differences in the attenuation rates at  $K_u$  and  $K_a$ -bands will further complicate retrieving drop size information from DFR measurements.

## 6. Concluding Remarks

[22] The results of this study point to the importance of accounting for nonsphericity of ice hydrometeors when retrieving characteristic particle size information from dual-frequency radar measurements at vertical incidence. Using the spherical particle model to develop techniques for sizing ice hydrometeors from dual-frequency radar measurements can produce biases in the retrieved information. While a spherical model is generally appropriate for calculating reflectivity factors of low density ice aggregate particles in the Rayleigh scattering regime, it becomes increasingly less adequate as hydrometeors reach sizes that are outside the Rayleigh regime. These theoretical findings were supported

by experimental data. The X-W-band DFR measurements from the airborne radar and collocated with these measurements estimates of characteristic ice cloud particle size indicated a better agreement with nonspherical model calculations for an aspect ratio of about 0.6–0.7 compared with spherical model results. Vertical incidence  $K_u$ - $K_a$ -band DFR in rain did not exhibit significant differences between spherical and equilibrium drop shape models.

[23] **Acknowledgment.** This study was supported in part by the CloudSat project and the Office of Science, U.S. Department of Energy, Grant No. DE-FG02-05ER63954.

## References

- Atlas, D., M. Kerker, and W. Hitschfeld (1953), Scattering and attenuation by nonspherical atmospheric particles, *J. Atmos. Terr. Phys.*, **3**, 108–119.
- Barber, P., and C. Yeh (1975), Scattering of electromagnetic waves by arbitrarily shaped dielectric bodies, *Appl. Opt.*, **14**, 2864–2872.
- Bringi, V. N., and V. Chandrasekar (2001), *Polarimetric Doppler Radar*, 636 pp., Cambridge Univ. Press, New York.
- Dungey, C. E., and C. F. Bohren (1993), Backscattering by nonspherical hydrometeors as calculated by the coupled-dipole method: An application in radar meteorology, *J. Atmos. Oceanic Technol.*, **10**, 526–532.
- Heymsfield, A. J., Z. Wang, and S. Y. Matrosov (2005), Improved radar ice water content retrieval algorithms using coincident microphysical and radar measurements, *J. Appl. Meteorol.*, **44**, in press.
- Hogan, R. J., A. J. Illingworth, and H. Sauvageot (2000), Measuring crystal size in cirrus using 35- and 94-GHz radars, *J. Atmos. Oceanic Technol.*, **17**, 27–37.
- Iguchi, T., R. Oki, E. A. Smith, and Y. Furuhashi (2002), Global precipitation measurement program, and the development of dual-frequency precipitation radar, *J. Commun. Res. Lab.*, **49**, 37–45.
- Korolev, A., and G. Isaac (2003), Roundness and aspect ratio of particles in ice clouds, *J. Atmos. Sci.*, **60**, 1795–1808.
- Matrosov, S. Y. (1992), Radar reflectivity in snowfall, *IEEE Trans. Geosci. Remote Sens.*, **30**, 454–461.
- Matrosov, S. Y. (1993), Possibilities of cirrus particle sizing from dual-frequency radar measurements, *J. Geophys. Res.*, **98**, 20,675–20,683.
- Matrosov, S. Y. (1998), A dual-wavelength radar method to measure snowfall rate, *J. Appl. Meteorol.*, **37**, 1510–1521.
- Matrosov, S. Y., R. F. Reinking, R. A. Kropfli, B. E. Martner, and B. W. Bartram (2001), On the use of radar depolarization ratios for estimating shapes of ice hydrometeors in winter clouds, *J. Appl. Meteorol.*, **40**, 479–490.
- Matrosov, S. Y. (2005), Attenuation-based estimates of rainfall rates aloft with vertically-pointing  $K_a$ -band radars, *J. Atmos. Oceanic Technol.*, **22**, 43–54.
- Matrosov, S. Y., R. F. Reinking, and I. V. Djalalova (2005), Inferring fall altitudes of pristine dendritic crystals from polarimetric radar data, *J. Atmos. Sci.*, **62**, 241–250.
- Mishchenko, M. I., J. W. Hovenier, and L. D. Travis (Eds.) (2000), *Light Scattering by Nonspherical Particles: Theory, Measurements and Applications*, 690 pp., Elsevier, New York.
- Mitchell, D. L. (1996), Use of mass- and area-dimensional power laws for determining precipitation particle terminal velocities, *J. Atmos. Sci.*, **53**, 1710–1723.
- Sekelsky, S. M., W. L. Ecklund, J. M. Firda, K. S. Gage, and R. E. McIntosh (1999), Particle size estimation in ice phase clouds using multifrequency reflectivity measurements at 95, 33, and 2.8 GHz, *J. Appl. Meteorol.*, **38**, 5–28.
- Stephens, G. L., and the CloudSat Science Team (2002), The CloudSat mission and the A-train. A new dimension of space-based observations of clouds and precipitation, *Bull. Am. Meteorol. Soc.*, **83**, 1771–1790.

A. J. Heymsfield, National Center for Atmospheric Research, Boulder, CO 80307, USA.

S. Y. Matrosov, Cooperative Institute for Research in Environmental Sciences, University of Colorado and NOAA ETL, Boulder, CO 80303, USA. (sergey.matrosov@noaa.gov)

Z. Wang, Department of Atmospheric Sciences, University of Wyoming, Laramie, WY 82071, USA.